Photocatalytic functional coatings of TiO$_2$ thin films on polymer substrate by plasma enhanced atomic layer deposition

Chang-Soo Lee [a], Jungwon Kim [b], J.Y. Son [a], Wonyong Choi [b], Hyungjun Kim [a,*]

[a] Department of Materials Science and Engineering, Pohang University of Science and Technology (POSTECH), Pohang 790-784, Republic of Korea
[b] School of Environmental Science and Engineering, Pohang University of Science and Technology (POSTECH), Pohang 790-784, Republic of Korea

ARTICLE INFO

ABSTRACT

We prepared photocatalytic TiO$_2$ thin films which exhibited relatively high growth rate and low impurity on polymer substrate by plasma enhanced atomic layer deposition (PE-ALD) from Ti(NMe$_2$)$_4$ [tetrakis (dimethylamido) Ti, TDMAT] and O$_2$ plasma to show the self-cleaning effect. The TiO$_2$ thin films with anatase phase and bandgap energy about 3.3 eV were deposited at growth temperature of 250 °C and the photocatalytic effects were compared with commercial Activ glass. From contact angles measurement of water droplet and photo-induced degradation test of organic liquid, TiO$_2$ thin films with anatase phases showed superhydrophilic phenomena and decomposed organic liquid after UV irradiation. The anatase TiO$_2$ thin film on polymer substrate showed highest photocatalytic efficiency after 5 h UV irradiation. We attribute the highest photocatalytic efficiency of TiO$_2$ thin film with anatase structure to the formation of suitable crystalline phase and large surface area.

© 2009 Elsevier B.V. All rights reserved.

1. Introduction

As an excellent photocatalyst, TiO$_2$ has received considerable attention during the past decade due to its high photocatalytic activity, high chemical stability, low toxicity, and low cost. Under ultraviolet (UV) irradiation of photon energy equal to or higher than the bandgap energy of TiO$_2$, electron–hole pairs are generated in the TiO$_2$ films. The photogenerated holes in the valence band and the electrons in conduction band diffuse to the TiO$_2$ surface and they produce highly energetic hydroxyl radicals ($^\bullet$OH) and superoxide radical anions (O$_2^{\bullet-}$) which can oxidize organic molecules on the TiO$_2$ surface [1–4]. In addition, TiO$_2$ photocatalyst destroys bacteria and viruses in water [5–8] and induces hydrophilic surface under UV light [9,10]. Thus, TiO$_2$ photocatalysts are widely used in various fields, such as window glass, ceramic tiles, stainless steel and wall papers utilizing its self-cleaning [11,12], anti-fogging [9,10], antibacterial activities [5–8,13], and water or air purification [14,15].

Generally, TiO$_2$ has three different crystal structures: rutile (tetragonal), anatase (tetragonal), and brookite (tetragonal) [16,17]. Among these polymorphic structures, both rutile and anatase phase are widely investigated as a photocatalyst. The structures of both anatase and rutile consist of chains of TiO$_6$ octahedra, but lattice structures of two crystals are obviously different. The difference in lattice structure causes different mass densities (3.894 g/cm^3 for anatase and 4.250 g/cm^3 for rutile) and electronic bandgaps (3.3 eV for anatase and 3.1 eV for rutile). It is well known that the photocatalytic activities of the anatase phase are superior to those of the rutile phase since the former has a more negative conduction band edge potential (higher potential energy of photogenerated electrons) than the latter [3]. Thus, in terms of photocatalytic efficiency, obtaining a suitable crystalline phase and high specific area are important factors.

In view point of practical application, it is necessary to deposit TiO$_2$ thin films on various solid substrates such as glass, ceramic tiles, and plastics in order to use TiO$_2$ photocatalyst in industry fields. As an example, Activ glass produced by Pilkington Corp. is being used for building windows. Also, there are some reports on the TiO$_2$ coated window glass [18–20], ceramic tiles [21,22], and wall paper, which are used to help clean indoor or outdoor environments. However, TiO$_2$ coating on polymer substrate is still in the early stage of development compared to other substrates such as glass and ceramic tiles. Polymers have many benefits as substrates for photocatalytic coating, such as flexibility, low weight, impact resistance, and low cost. Also, they can be made into a wide range of shapes. Thus, photocatalytic coated polymers can be widely used in diverse areas from construction or automotive industry to food packaging, kitchen utensils, or toys. However, due to their relatively low thermal instability, the photocatalytic coating should be carried out with caution.

TiO$_2$ thin films have been deposited by a variety of deposition methods including sol–gel [23], spray pyrolysis [24], hydrothermal

synthesis [25], sputtering [20], chemical vapor deposition (CVD) [26], pulsed laser deposition (PLD) [27], and atomic layer deposition (ALD) [18,28]. Until now, sol–gel and sputtering have been main deposition techniques for TiO_2 thin films for low temperature preparation on polymer substrates [29–32]. However, there are no reports on CVD or ALD TiO_2 on polymer substrates due to the required high growth temperature for crystallization of TiO_2. Generally, in case of CVD or ALD, substrate temperature above 300 °C is needed to crystallize the TiO_2 thin films [26,33,34]. ALD has several advantages over other deposition methods such as good film quality, accurate thickness control, excellent conformality, and uniformity over large areas, since ALD is characterized by the alternate exposure of chemical species with self-limiting surface reactions. Due to the surface reaction limited mechanism during growth, ALD produces high performance coating at lower growth temperature than CVD. Also, ALD has a benefit of producing very thin coating over complicated shape substrates, which is a big advantage for photocatalytic functional coating for various applications. Meanwhile, plasma-enhanced ALD (PE-ALD) has more benefits than thermal ALD such as improved film properties, high growth rate, and possibility of deposition at reduced substrate temperatures [35]. Thus, a suitable PE-ALD process may solve the high temperature degradation problem of polymer substrates and be a very effective method for the preparation of TiO_2 thin films on polymer substrates.

So far, ALD coating on polymer substrates has been rarely reported let alone PE-ALD TiO_2 as a photocatalyst on polymer substrate. Only a few researches about ALD of Al_2O_3 on polymer substrate were reported [36,37]. Since photocatalytic functional coatings of TiO_2 on polymer substrates need low temperature crystallization and high growth rate for mass production compatibility, it is necessary to study PE-ALD process of TiO_2 thin films and their photocatalytic activities in order to make highly efficient photocatalysts, which can reduce energy and time for production.

In our previous researches, we studied both thermal and PE-ALD process of TiO_2 thin films on Si (0 0 1) and stainless steel from a representative alkylamide precursor, $Ti(NMe_2)_4$ [tetrakis (dimethylamido) Ti, TDMAT] using water and oxygen plasma, respectively [38]. We obtained quite pure anatase and rutile TiO_2 thin films above 300 °C, which showed good photocatalytic activities such as superhydrophilicity and photo-induced decomposition of organic liquid. In this study, we prepared TiO_2 thin films on polymer substrates by PE-ALD and analyzed self-cleaning effects using a contact angle measurement and photo-degradation test of organic liquid, 4-chlorophenol (4-CP), under UV irradiation. The results confirmed that PE-ALD TiO_2 thin films on polymer substrates showed superhydrophilic surfaces and decomposed 4-CP aqueous solution under UV irradiation and their photocatalytic efficiency was much better than that of Activ glass.

2. Experimental

A home-made cold wall type remote PE-ALD chamber was used for this study. Sample sizes up to 200 mm in diameter can be loaded in the chamber, which is pumped by a turbomolecular pump producing a working base pressure of middle 10^{-6} Torr. The sample was heated using a resistive heating plate, providing growth temperatures of up to 500 °C. The temperature was measured using a thermocouple attached to the heater, and calibrated against another thermocouple attached to the sample. For PE-ALD process of TiO_2 thin films, TDMAT and O_2 plasma were used as a Ti precursor and O reactant, respectively. The TDMAT was contained in a bubbler and the bubbler was remained at room temperature without the use of a carrier gas due to its high enough vapor pressure. Oxygen was flown into a RF plasma source, which consists of a quartz tube wrapped with a multiple-turn coil set. RF

plasma power up to 600 W of 13.56 MHz can be provided; constant power of 300 W was used for this study. The flow rate of oxygen controlled by MFC was set at 30 sccm, resulting in 20 mTorr of working pressure. The chamber was purged by 50 sccm Ar gas between the precursor and the reactant exposure step.

TiO_2 thin films were prepared on 15 mm × 15 mm Kapton (polyimide) sheet. Before introduction into the PE-ALD chamber, an organic wet cleaning (ethanol and deionized water) was carried out in an ultrasonic bath, followed by nitrogen drying. Lastly, in order to evaporate alcohol and water absorbed by polymers, samples were heated at 100 °C for 1 h.

The growth temperature of TiO_2 thin film was below 250 °C for the temperature stability of polymer substrate. So, we chose 150 °C, 200 °C, and 250 °C for the experiments and composed 4-essential ALD steps such as TDMAT exposure – purging – O_2 plasma exposure – purging. The time of each process sequence consists of a 1 s pulse of TDMAT, 5 s of Ar purge, 2 s pulse of O_2 plasma, and 6 s of Ar purge. At TDMAT exposure step, TDMAT was introduced into the chamber and TDMAT molecules adsorb onto the substrate surface. And remained TDMAT molecules were evacuated during purge step. And then, at O_2 plasma exposure step, Ti–N bonding was broken and Ti instantly reacted with O to form a TiO_2 atomic layer. And then, remained O_2 and byproducts such as NO_x, CO_2 and H_2O were evacuated. This overall process can be described by following equation: $Ti(NMe_2)_4 + O_2$ plasma $\rightarrow TiO_2$ + byproducts (NO_x, CO_2, H_2O, etc.). This PE-ALD process sequence was repeated for 500 cycles. After TiO_2 thin film deposition, the thickness and optical absorption spectrum of the film were measured by ellipsometry. And then, we checked the adhesion strength through solvent treatment using water. The impurity contents and binding structures of the films were analyzed by X-ray photoemission spectroscopy (XPS). The crystal structures were determined by a glancing angle X-ray diffraction (GAXRD) with 1° of incident angle for all samples. Atomic force microscopy (AFM) was used to investigate the surface morphology and the surface roughness of the films and Activ glass.

The contact angle of water on TiO_2 thin film surface and photo-induced decomposition of organic liquid as a function of UV irradiation time were measured to observe the self-cleaning effects of the TiO_2 thin film on polymer substrate. In these experiments, we used Pilkington Activ glass for comparison. For the measurement of contact angle, Black Light Blue lamp (BLB, 10 W, wave length: 350–400 nm) was used as a light source and the exposure time range was 5–40 min. To observe the photocatalytic activity of TiO_2 thin film, the degradation rates of 4-CP under UV irradiation was monitored. The initial concentration of 4-CP was 0.1 mM and TiO_2 thin films were soaked in 4-CP solution and exposed with a 300 W Xe arc lamp (Oriel) as a light source. Light passes through an IR filter and UV cut-off filter ($\lambda > 324$ nm), and then the filtered light is focused onto an 11 mL Pyrex reactor. An incident light intensity was measured using a power meter (Newport 1830-C) and determined to be about 480 mW/cm^2 in the wavelength range of 324–420 nm. Upon UV irradiation, samples were withdrawn by a 1 mL syringe. And then identification and quantification of 4-CP were performed by using high performance liquid chromatography (HPLC).

3. Results and discussion

After PE-ALD of TiO_2 thin films on polymer substrates, the thicknesses of the films were measured by ellipsometry. The films grown at each deposition temperature showed similar thicknesses around 90 nm. From these results, we estimated that the growth rates of TiO_2 films were 1.8 Å/cycle which were much higher than those of other precursors including methoxide (0.6 Å/cycle) [18]

and chloride (0.5 Å/cycle) [39]. However, Aarik et al. reported a similar growth rate for thermal ALD TiO$_2$ from TiI$_4$ and H$_2$O (1.8 Å/cycle) [40].

The adhesion strength between TiO$_2$ film and polymer substrate was checked by solvent treatment using water for 24 h. During this experiment, we did not observe the film strip and we also did not detect any film strips during photocatalytic decomposition test for 4-CP under UV irradiation even though TiO$_2$ films were soaked in liquids like 4-CP for 5 h. From these results, we inferred that the adhesion strength of TiO$_2$ thin film on polymer substrate is enough to show their self-cleaning effects. Similar adhesion analysis was reported by Yang et al. [31]. They reported dip-coating of TiO$_2$ films on acrylonitrile–butadiene–styrene polymer (ABS) or polystyrene (PS) and checked the adhesion strength and abrasion resistance through solvent treatment using water and ethanol. They immersed TiO$_2$ films in water and ethanol for 24 h, and they did not observe the peeling of TiO$_2$ layers, meaning that the strong adherence of TiO$_2$ layer to polymer substrate.
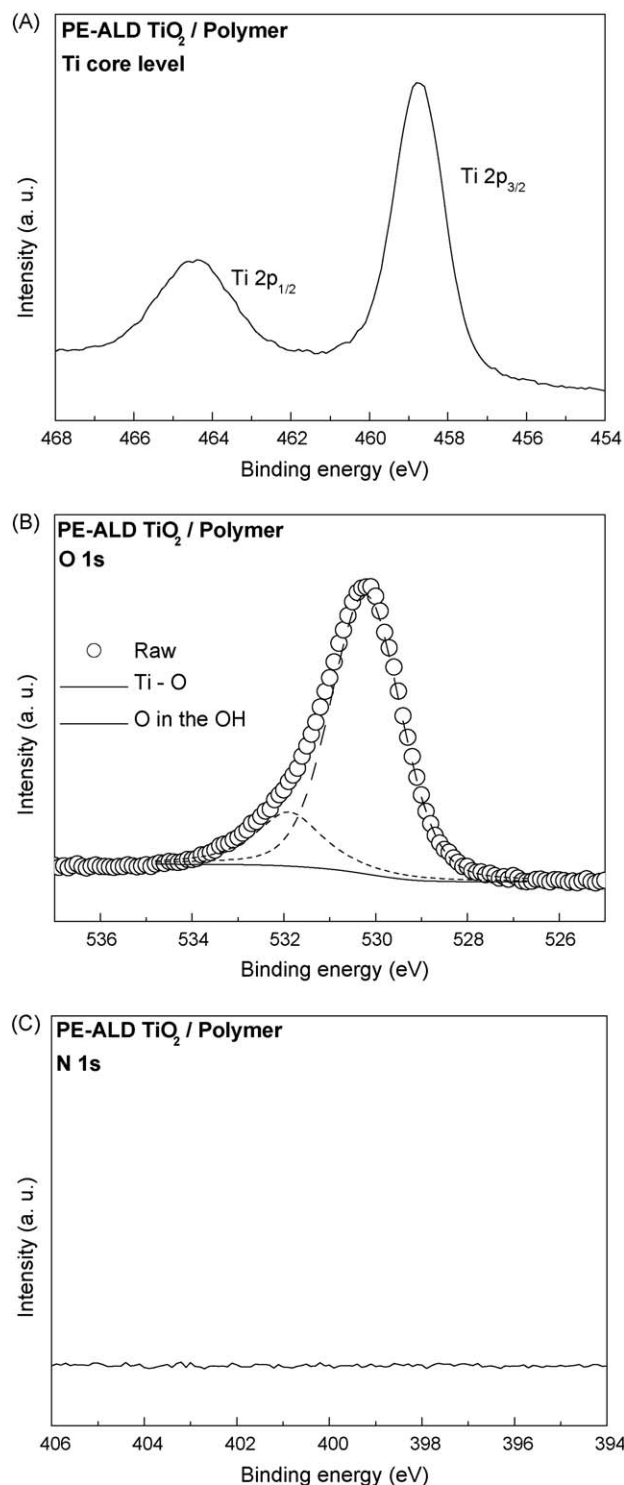
The X-ray diffraction (XRD) patterns of these TiO$_2$ thin films are shown in Fig. 1. Unlike film growth rate, the crystallinity of TiO$_2$ thin films largely depends on the deposition temperature. The films grown at temperatures at or below 200 °C were amorphous judging from the absence of any diffraction peaks, while the film grown at temperature of 250 °C consist of only anatase phase. Namely, the crystalline phase of TiO$_2$ thin films changed from amorphous to anatase phase with increasing growth temperature. Cheng and Chen [41] reported similar XRD results for ALD TiO$_2$ thin film from TiCl$_4$ and H$_2$O. They reported that TiO$_2$ films grown at temperature range from 200 °C to 300 °C showed only anatase phase XRD peaks.

XPS spectra of Ti 2p, O 1s and N 1s core levels for PE-ALD TiO$_2$ films grown at 250 °C are shown in Fig. 2(a)–(c) in order to analyze the chemical composition and the binding structure of TiO$_2$ thin films on polymer substrates. From Fig. 2(a), only pure Ti–O bond related XPS peaks were observed at Ti 2p$_{2/3}$ (located at 458.8 eV) and Ti 2p$_{1/2}$ (located at 464.3 eV), which have peak separation of 5.5 eV, indicating the presence of Ti^{4+} (TiO$_2$) in this film and no existence of Ti–N compound, which might have been formed by the contamination from the precursor ligands, and metallic Ti. By the deconvolution of the O 1s spectra, two O related peaks are observed. The peak at 530.2 eV is associated with pure TiO$_2$ [42] and the shoulder around 531.9 eV is attributed to the O in the OH group [43]. The N 1s spectrum in Fig. 2(c) shows no signal related to nitrogen in spite of using amide precursor for the current
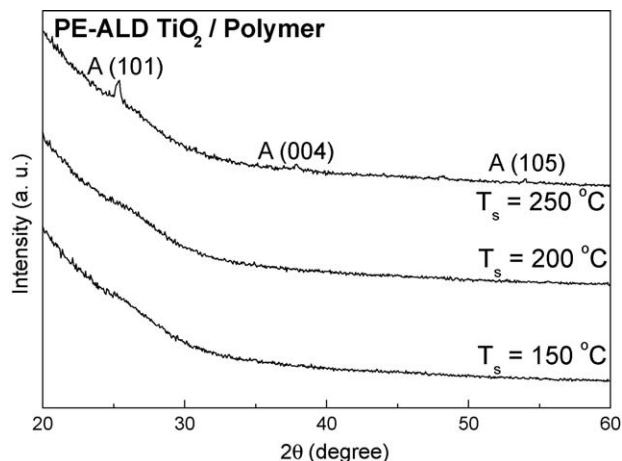
experiments. Thus, we inferred that the TiO$_2$ thin film on polymer substrate is quite pure.

To analyze the optical bandgap energies of PE-ALD TiO$_2$ thin films on polymer substrates, optical absorption spectra were obtained by ellipsometry. Optical absorption coefficient, α, has the following energy dependence [44]:

$$\alpha = \frac{2nk}{\lambda} = A(h\nu - E_g)^m,$$

Fig. 1. XRD spectra of PE-ALD TiO$_2$ thin films on polymer substrate as a function of growth temperature.

Fig. 2. XPS data for (a) Ti 2p, (b) O 1s, and (c) N 1s of the PE-ALD TiO$_2$ thin films on polymer substrate deposited at 250 °C.

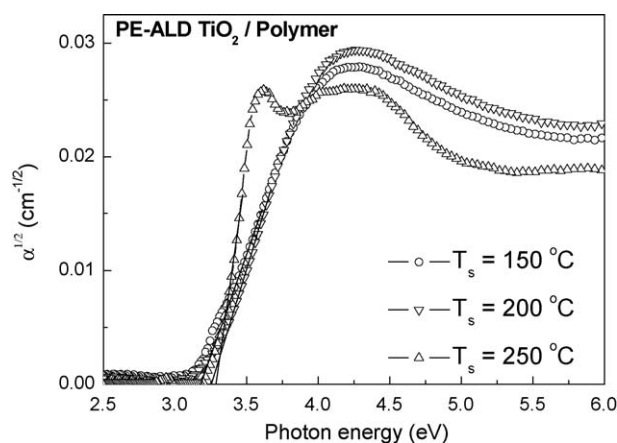**Fig. 3.** Optical absorption spectrum of TiO$_2$ thin films on polymer substrate grown at different substrate temperatures.

Fig. 5. Decomposition of 4-CP for TiO$_2$ thin films deposited at each growth temperature and Activ glass as a function of UV irradiation time.

where A is a constant, n is refractive index, k is extinction coefficient, $h\nu$ is the photon energy, and m is a constant equal to 1/2 and 2 for direct and indirect bandgap semiconductor, respectively. The bandgap energies of films were estimated by plotting $\alpha^{1/2}$ versus E ($h\nu$) as shown in Fig. 3. The bandgap energy of anatase TiO$_2$ thin film is 3.3 eV, in good agreement with a previous report [16], while the bandgap energy of amorphous TiO$_2$ thin films is around 3.2 eV which is little bit smaller than that of anatase film. All these results show that TiO$_2$ thin film with suitable polycrystalline phase for photocatalytic application with low impurities and generally known optical bandgap energy is deposited on polymer substrate at the growth temperature of 250 °C.

Fig. 4 shows the contact angle of water droplet on the TiO$_2$ thin films as a function of UV irradiation time. The initial contact angles of amorphous TiO$_2$ thin films deposited at 150 °C and 200 °C are about 57° and 73°, respectively, while those of anatase TiO$_2$ thin films and Activ glass are about 86° and 45°, respectively. After the irradiation of UV light for 40 min, the contact angles on amorphous TiO$_2$ thin films are not changed largely, only decrease down to around 50° without showing the superhydrophilicity. On the other hand, the contact angles of water on anatase TiO$_2$ thin films rapidly decrease and finally approach 5° after the exposure time of 20 min. The contact angles of Activ glass also gradually decrease and finally approach 5° after 30 min of UV irradiation. Thus, the polycrystalline PE-ALD TiO$_2$ thin films with anatase phase and Activ glass have the superhydrophilic surfaces.
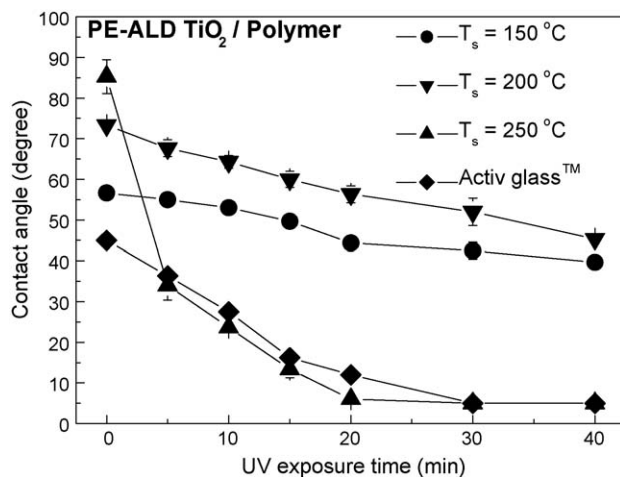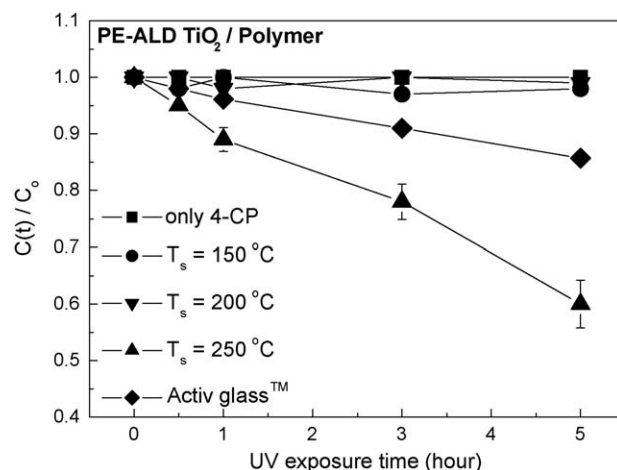

Fig. 4. Contact angles of water on TiO$_2$ thin films deposited at each growth temperatures and Activ glass as a function of UV irradiation time.

There are several reports on the superhydrophilicity of TiO$_2$ thin films [9,10]. Recently, Pore et al. [45] reported similar superhydrophilicity of ALD TiO$_2$ thin films on soda lime and borosilicate glass. The mechanism of hydrophilicity is different from that of photocatalytic decomposition, although the photogenerated electrons and holes are involved in both cases. Wang et al. [9,10] reported that the surface hydrophilicity of anatase and rutile TiO$_2$ thin films is independent of their photocatalytic activities and they explained that this effect occurs due to the production of oxygen vacancies on the TiO$_2$ surface during UV irradiation. After the generation of electron–hole pairs during UV irradiation, the electrons reduce the Ti (IV) cations to Ti (III) states and the holes oxidize O$_2^-$ anions. In this process, oxygen atoms are ejected from TiO$_2$ surface and oxygen vacancies are created. Then, these oxygen vacancies are supposed to interact strongly with water molecules, producing adsorbed OH groups and resulting in the hydrophilicity of TiO$_2$ surface.

To evaluate the photocatalytic efficiency of TiO$_2$ thin films on polymer substrate, the photo-induced degradation of 4-CP were measured under UV irradiation. For comparison, the photocatalytic activity of Activ glass was also measured. Fig. 5 shows the concentration changes of 4-CP liquid as a function of UV irradiation time. For 4-CP liquid and the amorphous TiO$_2$ thin films, no decomposition of 4-CP is observed after UV irradiation. However, anatase TiO$_2$ thin film and Activ glass show noticeable concentration decrease of 4-CP. They decomposed about 40% and 15% of 4-CP aqueous solution, respectively, after 5 h of UV irradiation. The highest photocatalytic activity of TiO$_2$ thin films was obtained for anatase TiO$_2$ thin film on polymer substrate, which was deposited at 250 °C. This result indicates that the crystalline phase of TiO$_2$ thin film is one of the most important factors to improve the photocatalytic efficiency of TiO$_2$. As mentioned above, anatase phase of TiO$_2$ which has larger bandgap energy is more suitable for higher photocatalytic activities.

AFM analysis of polymer substrate, TiO$_2$ thin film on polymer substrate and Activ glass was performed to show the surface morphology and roughness change before and after the TiO$_2$ ALD process and to compare the surface areas which related to surface roughnesses. As shown in Fig. 6(a) and (b), the surface roughnesses of polymer substrate and TiO$_2$ thin film are around 14.3 nm and 14.5 nm. This result indicates that TiO$_2$ thin film was deposited conformally on polymer substrate and the surface roughness of the TiO$_2$ coated surface was not changed during the ALD procedure. From Fig. 6(b) and (c), the surface roughnesses of PE-ALD TiO$_2$ thin films on polymer substrate and Activ glass are around 14.5 nm and

(a) Polymer substrate

(b) PE-ALD TiO$_2$ / Polymer

(c) Activ glass™ (TiO$_2$ / Glass)
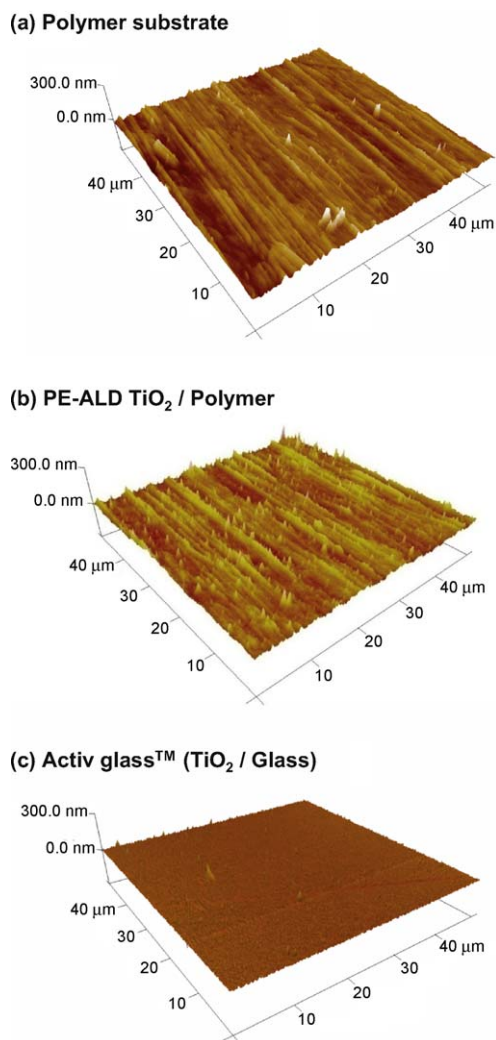
Fig. 6. AFM images of (a) polymer substrate, (b) TiO$_2$ thin films on polymer substrate and (c) Activ glass.

6.3 nm, respectively. We estimated that TiO$_2$ thin films on polymer substrate have larger surface area than Activ glass which affects the higher photocatalytic efficiency of TiO$_2$ thin films on polymer substrate. Thus, we suggest that the highest photocatalytic efficiency of anatase TiO$_2$ thin film was attributed to a suitable phase of TiO$_2$ thin film and larger surface area of the film which originated from larger surface roughness of the polymer substrate.

4. Conclusion

PE-ALD TiO$_2$ thin films with relatively high growth rate and low impurity were deposited on polymer substrate using TDMAT and O$_2$ plasma. The crystalline phase of TiO$_2$ thin films depends on the growth temperatures. From XRD analysis, the films deposited below 200 °C have amorphous phase. While TiO$_2$ thin film grown at 250 °C has anatase phase and this film has optical bandgap energy about 3.3 eV which is well known value in previous report. The surface roughnesses of TiO$_2$ thin films on polymer substrate are about 14.5 nm which is higher than that of Active glass, resulting in larger surface area which affects higher photocatalytic activity of TiO$_2$ thin film on polymer substrate. The contact angles of water and the decomposition of 4-CP under UV irradiation were measured to confirm the self-cleaning effect of TiO$_2$ thin films on polymer substrate. Photocatalytic effects of a commercial product, Activ glass, were also measured using the contact angle of water

and the decomposition of 4-CP for comparison. TiO$_2$ thin films with anatase phase and Activ glass showed superhydrophilic phenomena and decomposed 4-CP under UV irradiation. The anatase TiO$_2$ thin film on polymer substrate showed highest photocatalytic activity after 5 h UV irradiation. We suggest that the suitable phase of TiO$_2$ and large surface area are main factors for the highest photocatalytic efficiency of TiO$_2$ thin film deposited at 250 °C.

References

[1] A. Fujishima, K. Honda, Nature 238 (1972) 37–38.
[2] A. Heller, Accounts of Chemical Research 28 (1995) 503–508.
[3] A. Fujishima, T.N. Rao, D.A. Tryk, Journal of Photochemistry and Photobiology C: Photochemistry Reviews 1 (2000) 1–21.
[4] C. Kormann, D.W. Bahnemann, M.R. Hoffmann, Environmental Science & Technology 25 (1991) 494–500.
[5] R.J. Watts, S. Kong, M.P. Orr, G.C. Miller, B.E. Henry, Water Research 29 (1995) 95–100.
[6] K. Sunada, Y. Kikuchi, K. Hashimoto, A. Fujishima, Environmental Science & Technology 32 (1998) 726–728.
[7] K. Sunada, T. Watanabe, K. Hashimoto, Journal of Photochemistry and Photobiology A: Chemistry 156 (2003) 227–233.
[8] P.-C. Maness, S. Smolinski, D.M. Blake, Z. Huang, E.J. Wolfrum, W.A. Jacoby, Applied and Environmental Microbiology 65 (1999) 4094–4098.
[9] R. Wang, K. Hashimoto, A. Fujishima, M. Chikuni, E. Kojima, A. Kitamura, M. Shimohigoshi, T. Watanabe, Nature 388 (1997) 431–432.
[10] R. Wang, K. Hashimoto, A. Fujishima, M. Chikuni, E. Kojima, A. Kitamura, M. Shimohigoshi, T. Watanabe, Advanced Materials 10 (1998) 135–138.
[11] Y. Paz, Z. Lou, L. Rabenberg, A. Heller, Journal of Materials Research 10 (1995) 2842–2848.
[12] Y. Ohko, S. Saitoh, T. Tatsuma, A. Fujishima, Journal of the Electrochemical Society 148 (2001) B24–B28.
[13] P. Evans, D.W. Sheel, Surface and Coatings Technology 201 (2007) 9319–9324.
[14] J. Peral, X. Domenech, D.F. Ollis, Journal of Chemical Technology and Biotechnology 70 (1997) 117–140.
[15] J.A. Byrne, B.R. Eggins, N.M.D. Brown, B. McKinney, M. Rouse, Applied Catalysis B: Environmental 17 (1998) 25–36.
[16] A.L. Linsebigler, G. Lu, J.T. Yates Jr., Chemical Reviews 95 (1995) 735–758.
[17] S.-D. Mo, W.Y. Ching, Physical Review B 51 (1995) 13023–13032.
[18] V. Pore, A. Rahtu, M. Leskel, M. Ritala, T. Sajavaara, J. Keinonen, Chemical Vapor Deposition 10 (2004) 143–148.
[19] T. Watanabe, A. Nakajima, R. Wang, M. Minabe, S. Koizumi, A. Fujishima, K. Hashimoto, Thin Solid Films 351 (1999) 260–263.
[20] S. Takeda, S. Suzuki, H. Odaka, H. Hosono, Thin Solid Films 392 (2001) 338–344.
[21] P.S. Marcos, J. Marto, T. Trindade, J.A. Labrincha, Journal of Photochemistry and Photobiology A: Chemistry 197 (2008) 125–131.
[22] S. Kato, S. Kato, H. Taoda, S. Katoh, High Pressure Research 20 (2001) 415–419.
[23] J. Yu, X. Zhao, Q. Zhao, Thin Solid Films 379 (2000) 7–14.
[24] M.O. Abou-Helal, W.T. Seeber, Applied Surface Science 195 (2002) 53–62.
[25] J.H. Lee, M. Kang, S.-J. Choung, K. Ogino, S. Miyata, M.-S. Kim, J.-Y. Park, J.-B. Kim, Water Research 38 (2004) 713–719.
[26] A. Mills, N. Elliott, I.P. Parkin, S.A. O'Neill, R.J. Clark, Journal of Photochemistry and Photobiology A: Chemistry 151 (2002) 171–179.
[27] Y. Suda, H. Kawasaki, T. Ueda, T. Ohshima, Thin Solid Films 453–54 (2004) 162–166.
[28] R. Pheamhom, C. Sunwoo, D.-H. Kim, Characteristics of Atomic Layer Deposited TiO$_2$ Films and their Photocatalytic Activity, 4th ed., AVS, 2006, pp. 1535–1539.
[29] M. Langlet, A. Kim, M. Audier, J.M. Herrmann, Journal of Sol–Gel Science and Technology 25 (2002) 223–234.
[30] J.O. Carneiro, V. Teixeira, A. Portinha, A. Magalhãs, P. Coutinho, C.J. Tavares, R. Newton, Materials Science and Engineering: B 138 (2007) 144–150.
[31] J.-H. Yang, Y.-S. Han, J.-H. Choy, Thin Solid Films 495 (2006) 266–271.
[32] M. Langlet, A. Kim, M. Audier, C. Guillard, J.M. Herrmann, Thin Solid Films 429 (2003) 13–21.
[33] J. Aarik, A. Aidla, T. Uustare, V.N. Sammelselg, Journal of Crystal Growth 148 (1995) 268–275.
[34] M. Ritala, M. Leskela, L. Niinisto, P. Haussalo, Chemistry of Materials 5 (1993) 1174–1181.
[35] H. Kim, H.-B.-R. Lee, W.J. Maeng, Thin Solid Films 517 (2009) 2563–2580.
[36] C.A. Wilson, R.K. Grubbs, S.M. George, Chemistry of Materials 17 (2005) 5625–5634.

[37] X. Liang, S.M. George, A.W. Weimer, N.-H. Li, J.H. Blackson, J.D. Harris, P. Li, Chemistry of Materials 19 (2007) 5388–5394.
[38] W.J. Maeng, H. Kim, Electrochemical and Solid-State Letters 9 (2006) G191–G194.
[39] H. Kawakami, R. Ilola, L. Straka, S. Papula, J. Romu, H. Hanninen, R. Mahlberg, M. Heikkila, Journal of the Electrochemical Society 155 (2008) C62–C68.
[40] J. Aarik, A. Aidla, T. Uustare, K. Kukli, V.N. Sammelselg, M. Ritala, M. Leskel, Applied Surface Science 193 (2002) 277–286.
[41] H.E. Cheng, C.C. Chen, Journal of the Electrochemical Society 155 (2008) D604–D607.
[42] Y. Cheng, H. Sun, W. Jin, N. Xu, Chemical Engineering Journal 128 (2007) 127–133.
[43] D. Wang, Y. Wang, X. Li, Q. Luo, J. An, J. Yue, Catalysis Communications 9 (2008) 1162–1166.
[44] P.M. Kumar, S. Badrinarayanan, M. Sastry, Thin Films 358 (2000) 122–130.
[45] V. Pore, T. Kivel, M. Ritala, M. Leskel, Dalton Transactions (2008) 6467–6474.